Published in final edited form as:
Br J Haematol. 2011 October ; 155(1): 111–121. doi:10.1111/j.1365-2141.2011.08805.x.

Membrane Compartmentalization in Southeast Asian Ovalocytosis Red Blood Cells

Rossen Mirchev[1], **Alexander Lam**[2,3], and **David E. Golan**[1,4]

[1]Department of Biological Chemistry and Molecular Pharmacology, Harvard Medical School, Boston, Massachusetts

[2]Harvard Medical School, Boston, MA

[4]Hematology Division, Brigham and Women's Hospital, Boston, Massachusetts

Summary

Red blood cells (RBCs) from individuals with Southeast Asian ovalocytosis (SAO) contain a mutant band 3 protein that causes the formation of unique linear oligomers in the RBC membrane. We used single-particle tracking to measure the lateral diffusion of individual glycophorin C (GPC), band 3, and CD58 proteins in membranes of intact SAO RBCs and normal RBCs (nRBCs). GPC, an integral protein that binds with high affinity to the RBC membrane skeleton, showed oscillatory motion within confinement areas that were smaller in SAO RBCs than in nRBCs. The additional confinement in SAO RBCs could be due to membrane stiffening associated with the SAO phenotype. Band 3 in both SAO RBCs and nRBCs also showed confined motion over short times (ms) and distances (nm), and the area of confinement was smaller in SAO RBCs than in nRBCs. These data presumably reflect the constraints imposed by band 3 oligomerization. Similarly, the glycosylphosphatidylinositol-linked protein CD58 showed loosely confined diffusion in nRBCs and a substantially higher degree of confinement in SAO RBCs. Restricted protein mobility could contribute to the altered adherence of parasite-infected RBCs to vascular endothelium that is thought to protect individuals with SAO from severe manifestations of malaria.

Keywords

red cells; Southeast Asian Ovalocytosis; protein diffusion; single-particle tracking

Introduction

In contrast to normal human red blood cells (RBCs), which exhibit a biconcave disc shape, RBCs from individuals with Southeast Asian ovalocytosis (SAO) have a large oval shape with a transverse band of pallor and sometimes a "double-slit" appearance (Bruce and Tanner 1999, Kay 2004, Lux and Palek 2003). This unique shape has been linked to a heterozygous deletion in band 3, the RBC chloride–bicarbonate anion exchanger that also serves as the principal anchoring protein for the RBC membrane skeleton (Liu, *et al* 1990).

Correspondence: David E. Golan, MD, PhD, Department of Biological Chemistry and Molecular Pharmacology, Harvard Medical School, 250 Longwood Avenue, SGMB 304, Boston, MA 02115, Tel: 617-432-2256, Fax: 617-432-3833, dgolan@hms.harvard.edu.
[3]Current address: Emergency Department, Davies Campus, California Pacific Medical Center, San Francisco, California;

Conflict of interest

The authors declare that there are no competing financial interests in relation to the work described in this paper.

Contribution: R.M., A.L., and D.E.G. designed research; R.M. and A.L. performed research; R.M. and D.E.G. analysed data; and R.M. and D.E.G. wrote the paper.

The SAO phenotype results from a 27-basepair deletion in the gene that encodes band 3 **(*SLC4A1*)**, which corresponds to a 9 amino-acid deletion in the protein (Mohandas, *et al* 1992). Specifically, the deletion involves residues 400–408 at the cytoplasmic end of the first transmembrane segment of band 3. Physiologically, the deletion renders the abnormal protein incapable of mediating chloride–bicarbonate exchange (Lux and Palek 2003, Schofield, *et al* 1992a). Structurally, the deletion allows band 3 to cause the formation of unique linear oligomers in the SAO RBC membrane (Liu, *et al* 1995). The homozygous form of SAO is lethal and the heterozygous form is clinically asymptomatic (Lux and Palek 2003, Schofield, *et al* 1992a), although cation permeability defects have been reported in SAO RBCs (Guizouarn, *et al* 2011). SAO RBCs contain approximately 50% normal band 3 molecules and 50% mutant band 3 molecules (Bruce, *et al* 2000, Liu, *et al* 1990). SAO RBCs are abnormally rigid (Mohandas, *et al* 1984), and this rigidity may underlie the association between the SAO phenotype and clinical resistance to cerebral malaria (Genton, *et al* 1995).

The normal RBC membrane is composed of two coupled substructures: an outer lipid bilayer, in which proteins of different sizes are embedded, and an inner protein network, the membrane skeleton, consisting of spectrin heterotetramers and short actin filaments in a triangular lattice arrangement (Lux and Palek 2003). Two major junctions are formed between the lipid bilayer and the membrane skeleton: (1) the band 3-glycophorin A-ankyrin complex (Bennett and Healy 2008); and (2) the glycophorin C (GPC)-protein 4.1-actin complex (Anong, *et al* 2009, Khan, *et al* 2008, Salomao, *et al* 2008). The integrity of the skeletal protein network and the linkages between the lipid bilayer and the membrane skeleton have important roles in determining membrane deformability and stability. SAO RBCs are reported to be 11–20 fold less deformable and 1.3- to 1.5-fold more stable than normal RBCs (Chasis and Mohandas 1986). Band 3 oligomerization in the SAO RBC membrane is thought to contribute to these alterations in membrane visco-elastic properties (Chasis and Mohandas 1986, Moriyama, *et al* 1992), because there is no evidence that the membrane skeleton is altered in SAO RBCs (Kuma, *et al* 2002, Wang 1994). Size-exclusion high performance liquid chromatography (HPLC) has demonstrated that band 3 exists in the normal RBC membrane in the form of homodimers, homotetramers, and a small fraction of higher-order oligomers. Band 3 dimers are the predominant species (~70%) (Casey and Reithmeier 1991). In contrast, SAO RBCs contain a higher proportion of band 3 tetramers (50%) along with the higher-order band 3 oligomers (Sarabia, *et al* 1993). Current models of the RBC membrane suggest three populations of band 3 molecules: (1) band 3 dimers that are not bound to the membrane skeleton; (2) band 3 tetramers bound to the ankyrin complex; and (3) band 3 bound to the GPC complex, which is suggested to be in dimeric form based on the stoichiometry of binding to adducin (Anong, *et al* 2009).

In this work, we used single-particle tracking (SPT) methods to measure the lateral diffusion of individual RBC membrane proteins labelled with antibody-conjugated gold beads. In general, the diffusion of these proteins in the viscous lipid environment can be constrained by: (1) diffusive collisions with the membrane skeleton or with other membrane proteins or lipids; or (2) direct binding interactions with transmembrane or membrane skeletal proteins. We studied the diffusion of three proteins — GPC, band 3, and CD58. GPC and band 3 are transmembrane proteins of 32 kDa and 90–100 kDa, respectively (Lux and Palek 2003). CD58 is a glycosylphosphatidylinositol (GPI)-linked protein of 64–73 kDa (Murphy, *et al* 2004). These proteins represent three types of molecules that are expected to have different diffusive properties in the normal RBC membrane and to be affected differently by the structural alterations in the SAO RBC membrane. Fluorescence photobleaching recovery (FPR) experiments showed that 40–70% of band 3 molecules are laterally mobile in the normal RBC membrane (Corbett, *et al* 1994), suggesting that the band 3 dimers are preferentially mobile and, thus, not associated with the membrane skeleton. Furthermore,

FPR studies of normal RBCs and spectrin-deficient RBCs from patients with hereditary spherocytosis and hereditary pyropoikilocytosis show that the lateral mobility of band 3 is primarily regulated by the RBC membrane skeleton (Corbett, *et al* 1994). The rotational mobility of normal band 3 is unaffected by changes in the RBC membrane skeleton (Corbett, *et al* 1994), although the rotational mobility of band 3 in SAO RBCs is decreased due to its tendency to form high-order oligomers (Liu, *et al* 1995). Here, we found that the diffusion properties of GPC, band 3, and CD58 in SAO RBCs were all significantly different from those in normal RBCs, showing smaller diffusion coefficients and more tightly confined motion. We also provided evidence that the mutant SAO band 3 oligomers introduce a novel mode of RBC membrane compartmentalization that affects molecular diffusion in the SAO RBC membrane.

Materials and methods

Preparation of normal and SAO RBCs

Fresh human blood was obtained after informed consent from 12 normal adult volunteers at Brigham and Women's Hospital, Boston, MA. Three samples were used for GPC measurements, four for band 3 measurements, and five for CD58 measurements. The variation in the results from the normal samples was not statistically significant for any of the three proteins (T-test).

Fresh blood was also obtained after informed consent from an individual with heterozygous SAO at Harvard Medical School, Boston, MA. This individual was not anaemic (haemoglobin, 151 g/l; haematocrit, 41.3%) and his RBCs were large (MCV, 100.2 fl) and ovalocytic. A minor fraction of his RBCs exhibited a "double-slit" appearance; these cells were excluded from use in single-particle tracking experiments.

Normal and SAO blood samples were centrifuged at 1500×g for 5 min. The plasma and buffy coat were discarded, and RBCs were washed three times in HBS (25 mM HEPES, pH 7.4, 118.8 mM NaCl, 6 mM KCl, 5 mM $MgCl_2$,1.2 mM NaH_2PO_4) at 500×g for 2 min. RBCs were resuspended at 10% haematocrit in HBS with 10 mM glucose and used in experiments within 12 h.

Preparation of Fab' fragments and conjugation to gold beads

Monoclonal anti-GPC (clone BRIC4, mouse IgG_1), anti-CD58 (clone BRIC5, mouse IgG_2), and anti-band 3 (clone BRIC6, mouse IgG_3) were purchased from the International Blood Group Reference Laboratory, Bristol, UK. Antibodies were fragmented using Fab' preparation kits (Pierce, Rockford, IL) by digestion with immobilized papain (BRIC5, BRIC6) or ficin (BRIC4) and separation on a protein A or protein G column. Non-specific Fab' fragments were prepared from mouse IgG_2 (Calbiochem, Rockland, MA).

A mixture of specific and non-specific Fab' fragments was conjugated to colloidal gold (40 nm beads; RDI, Flanders, NJ) by incubation for 4 min in 5 mM sodium phosphate buffer at pH 7.0. Polyethyleneglycol (PEG20k; Sigma, St. Louis, MO) was then added to a final concentration of 0.05% and mixed for 3 min. The gold beads were then centrifuged at 8,000×g for 10 min, and the supernatant was discarded. The gold beads were resuspended in HBS with 0.02% PEG20k and centrifuged for 10 min. The final suspension of gold beads had OD_{520} = 4. The optimum mixture of specific and non-specific Fab' fragments was determined by: first, determining the minimum amount of each Fab' fragment that completely covered the gold bead surface and protected from coagulation of the colloid in 100 mM sodium chloride (minimum protective amount, MPA); and second, titrating the amount of specific Fab' fragment added to the MPA of non-specific Fab' until cell labelling with gold beads was 5–10 fold greater than the background labelling.

Labelling of membrane proteins

Twenty μl of RBCs at 10% haematocrit were incubated with 5 μl of conjugated gold beads for 40 min at room temperature with mixing, and then washed twice and resuspended in HBS with 1% bovine serum albumin. The laelled RBCs were placed between a microscope slide and a cover slip to form samples that were 3–5 μm thick, sealed, and allowed to settle for 10 min before viewing. Two methods were used to verify the specificity of labelling: first, control samples were prepared using gold beads conjugated to the non-specific Fab' fragment alone; second, RBCs were incubated for 30 min with an excess of unconjugated specific Fab' fragment and then incubated with gold beads conjugated to the specific Fab' fragment.

Single-particle tracking system

The experimental apparatus included an inverted microscope (Eclipse TE300, Nikon, Melville, NY) equipped with differential interference contrast (DIC) optics (Mirchev and Golan 2001). Illumination was provided by a 100-W mercury arc lamp delivered through an optical fibre scrambler (Technical Video Port Townsend, WA). An oil-immersion 60×/1.4 NA objective and oil-immersion 1.4 NA condenser were used to view the sample. Images were recorded using a CCD video camera (Photron SR-Ultra; Photron, San Diego, CA) at 1000 frames per second (fps), and transferred to a computer for storage and analysis. Image noise filtering and tracking of bead motion were performed using MetaMorph (Molecular Devices, Sunnyvale, CA). Two-dimensional bead trajectories were analysed using C++ and MATLAB-based custom programs. The accuracy in the x,y-position measurement was determined to be 7 nm by measuring the standard deviation in x and y of 40-nm gold beads embedded in a 20% agarose gel.

Single-particle tracking analysis

The analysis of trajectories was based on the mean square distance (MSD) statistic:

$$MSD(\Delta t_n)=\frac{1}{\mathrm{N}-\mathrm{n}}\sum_{i=1}^{N-n}\left[(x_{i+n}-x_i)^2+(y_{i+n}-y_i)^2\right],$$

where x_i, y_i were the coordinates of the i-th position in the track; $\Delta t_n = n \times \delta; \delta$ was the time interval between successive images (δ=1 ms); and N was the total number of images (N=2000). Since the standard deviation of each MSD(Δt_n) point increased with n, only one-third of the time intervals in any given particle trajectory (i.e., from Δt_1 to $\Delta t_{N/3}$) were used in the analysis. Experimental MSD(Δt_n) points were fitted by least squares analysis to the general function for lateral (two-dimensional) diffusion:

$$MSD(t)=\mathrm{G}\,\mathrm{t}^{\alpha},$$

where G and α were fit parameters that described the rate and the type of motion (i.e., confined diffusion, unconfined (Brownian) diffusion, or directed motion) (Feder, *et al* 1996). A linear fit (α=1) to MSD($\Delta t_{n\,=\,1\text{ to }4}$) was used to estimate the diffusion coefficient of the laelled molecule over short times and distances, called the micro-diffusion coefficient, D_μ=G/4. D_μ can be interpreted as a diffusion process that is relatively unaffected by confinement barriers (Saxton 1995). The intersection of the linear fit with the ordinate (i.e., at Δt=0) was subtracted from all MSD(Δt_n) values to account for experimental noise.

Over longer time and distance scales, the motion of the laelled molecule reflected the presence of molecular obstacles such as integral membrane proteins or areas of membrane

lipid inhomogeneity, molecular confinement by barriers such as the membrane skeleton, or transient binding of the laelled protein to other integral proteins or skeletal proteins. The fit of MSD($\Delta t_{n=1 \text{ to } N/3}$) yielded the macro-diffusion coefficient, $D_M=G/4$, and the value of α, which was used to categorize the trajectories by type of motion. In cases of confined diffusion, the dimensions of the confinement in the x- and y-directions, L_x and L_y, were estimated from a nonlinear least squares fit to the following equation (Kusumi, *et al* 1993):

$$MSD_{x,y}(\Delta t_n)=\frac{{L_{x,y}}^2}{6}-\frac{16{L_{x,y}}^2}{\pi^4}\sum_{n=1(odd)}^{\infty}\frac{1}{n^4}\exp\left[-\left(\frac{n\pi}{L_{x,y}}\right)^2 D_\mu t\right].$$

Each membrane protein trajectory was analysed to obtain D_μ, D_M, α, L_x, and L_y. Diffusion trajectories were classified as ‘tightly confined’, ‘confined’, or ‘Brownian’ based on the population analysis described by Cairo et al. (2006). Briefly, a kernel-smoothing probability density calculation was used to smooth the normalized distribution of α values for each experimental condition. This envelope (smoothing) curve was fitted to the sum of three Gaussian distributions, which represented the three populations of trajectories. These Gaussians had independent means and standard deviations. According to Johnson et al. (1994), two normal distributions are statistically different if:

$$\frac{{\sigma_1}^2+{\sigma_2}^2}{{\sigma_1}^2{\sigma_2}^2}(\mu_1-\mu_2)^2>8,$$

where μ and σ denote the mean and standard deviation of each distribution. Trajectories with α values falling under the Gaussian curve with the lowest mean were classified as ‘tightly confined,’ trajectories with α values falling under the Gaussian curve with the highest mean (α~1) were classified as ‘unconfined (Brownian),’ and trajectories associated with the middle Gaussian curve were classified as ‘confined.’ The fractional percentage of each population was calculated from the normalized weighting factor by which each Gaussian was multiplied in the best-fit sum.

The motion of the membrane skeleton-linked protein GPC was approximated as the oscillation of a particle in a harmonic potential with a spring constant $\boldsymbol{k_{eff}}$. The spring constant was used to estimate the effective stiffness of the RBC membrane. For motion in a harmonic potential $E(x)$, where x was the position of the particle, the Boltzmann statistic yielded:

$$E(x)=-k_BT\ln p(x)+k_BT\ln C$$

where $p(x)$ was the probability density, k_B was the Boltzmann constant, T was the temperature, and C was a normalizing constant. Using the centre of mass of a given trajectory as the likely equilibrium position, x and its distribution $p(x)$ were calculated. Then, $E(x)$ was fitted with the function:

$$E(x)=k_{eff}\,x^2/2+constant,$$

where the spring constant $\boldsymbol{k_{eff}}$ was the fitted parameter.

Results

Population analysis

The experimental trajectories for each of the proteins — GPC, band 3, and CD58 — were classified into groups of distinctive diffusivity. Three populations were defined according to the α value of the trajectory (Fig 1). In each panel, the dark blue curve represents the envelope smoothing function calculated from the experimental data; the red curves are Gaussian best-fit curves denoting the deconvolved populations; and the green curve is the sum of the red curves. For all trajectories, it was observed that higher α values correlated with higher D_M values. The histogram of experimental values is shown in the background of each panel for comparison between conventional binning analysis and kernel density estimation (see Materials and methods).

For GPC in both normal and SAO RBCs, the three red curves differed statistically from one another, thus showing three populations of trajectories: 'tightly confined,' population peak 1, α = 0.10–0.30; 'confined,' population peak 2, α = 0.30–0.70; and 'unconfined or Brownian,' population peak 3, α = 0.70–1.10 (Fig 1A, Table 1). The magnitude of the α value of each population peak was statistically identical for nRBCs and SAO RBCs (Fig 1A, compare left and right panels). The fraction of trajectories in each population was calculated as described above and is shown in Table 1. The tightly confined population of GPC molecules in SAO RBCs was larger than the tightly confined population in nRBCs, and the confined and unconfined populations in SAO RBCs were correspondingly smaller.

Trajectories of band 3 laelled with BRIC6 showed three statistically different populations in both nRBCs and SAO RBCs (Fig 1B, Table 2). The tightly confined population of band 3 molecules in SAO RBCs was substantially larger than the tightly confined population in nRBCs, and the confined and unconfined populations in SAO RBCs were substantially smaller. A fraction of band 3 molecules showed α~1 in both nRBCs (29%) and SAO RBCs (20%), suggesting that some band 3 molecules were capable of diffusing in the membrane over long times and distances.

Three populations of trajectories of the GPI-linked protein CD58 were statistically different from one another and exhibited predominantly high α values in normal and SAO RBC membranes (Fig 1C, Table 3). The tightly confined population was larger in SAO RBCs (44%) than in nRBCs (27%), and the unconfined population was smaller in SAO RBCs (33%) than in nRBCs (48%).

Diffusion of GPC

There were three populations of GPC trajectories in both normal and SAO RBCs, but the fraction of molecules in each population was different for the two RBC types. Confined lateral diffusion was the major mode of motion in both nRBCs and SAO RBCs (Figs 2A, 2B); the fractions of confined and tightly confined trajectories summed to 89% and 94%, respectively (Table 1). A fraction of GPC molecules in normal (11%) and SAO RBCs (6%) was not laterally restricted (Table 1). The distribution of GPC diffusion parameters is shown in Fig 2C. D_μ was greater in normal RBCs than in SAO RBCs (mean values, 4.9×10^{-10} cm^2/s and 2.4×10^{-10} cm^2/s, respectively), as was D_M (mean values, 2.9×10^{-11} cm^2/s and 1.2×10^{-11} cm^2/s).

The confinement size of GPC was 90 nm in normal RBCs and 63 nm in SAO RBCs for the confined populations, and 62 nm and 53 nm for the tightly confined populations, respectively (Fig 2C, Table 1). None of the GPC molecules seemed to "leave" these confinement areas during the period of experimental observation (see Figs 2A, 2B). We propose that this motion is consistent with a GPC molecule that is tethered rather than

corralled (unpublished observations). If this is the case, then the smaller confinement size of GPC in SAO RBCs suggested that the SAO RBC membrane was stiffer than the normal RBC membrane. Figure 3 presents the distribution of values of the effective spring constant, k_{eff}, calculated from the GPC trajectories that showed laterally restricted motion. The distribution of k_{eff} values was wider and shifted to the right in SAO RBCs compared to normal RBCs (Fig 3), suggesting that GPC was bound more stiffly to the membrane skeleton in SAO RBCs.

Diffusion of band 3

Representative band 3 trajectories are shown in Figs 4A, 4B. Fifty percent of trajectories in normal RBCs and 77% of trajectories in SAO RBCs showed tight confinement, remaining localized in one region of the membrane over the entire period of observation (Fig 4A, Table 2). Although 20% of band 3 trajectories showed Brownian diffusion in SAO RBCs, only 3% of trajectories showed confined diffusion. The vast preponderance of tightly confined compared to confined trajectories in SAO RBCs suggested the presence of additional compartmentalization, which was probably imposed by band 3 oligomers (see Discussion). D_μ was smaller in SAO RBCs than in normal RBCs (mean values, 3.9×10^{-10} cm^2/s and 7.6×10^{-10} cm^2/s, respectively; Fig 4C). D_M was also smaller in SAO RBCs than in nRBCs (mean values, 3.4×10^{-11} cm^2/s and 10.1×10^{-11} cm^2/s, respectively). The distribution of confinement sizes was shifted to smaller values in SAO RBCs (Fig 4C, Table 2).

Using radioiodinated IgG and Fab fragments, Smythe, *et al* (1995) determined that the level of binding of BRIC6 anti-band 3 Fab fragments to SAO RBCs was decreased to 47% of its binding to nRBCs. Furthermore, although BRIC6 binds to normal band 3 expressed exogenously in *Xenopus* oocytes, this antibody fails to bind to mutant SAO band 3 expressed in oocytes. Together, these observations suggest that the BRIC6 epitope is concealed in mutant SAO band 3 (Groves, *et al* 1993). This property of BRIC6 suggests that the band 3 diffusion parameters reported above pertained only to normal band 3 molecules in both nRBCs and SAO RBCs (see also Supporting Information).

Diffusion of CD58

The fraction of CD58 trajectories showing unconfined motion was 48% in normal RBCs and only 33% in SAO RBCs (Table 3). Furthermore, the diffusion pattern of confined CD58 molecules was qualitatively different in nRBCs (Fig 5A) compared to that in SAO RBCs (Fig 5B). The motion of confined CD58 was noticeably more compartmentalized in SAO RBCs, suggesting the presence of different restriction mechanisms. Given that CD58 is localized to the outer leaflet of the lipid bilayer, the molecular constraints on CD58 motion were probably not due to differences in the normal and SAO membrane skeleton (see Discussion). D_μ was smaller in SAO RBCs than in normal RBCs (mean values, 3.9×10^{-10} cm^2/s and 6.3×10^{-10} cm^2/s, respectively), as was D_M (mean values, 5.4×10^{-11} cm^2/s and 15.7×10^{-11} cm^2/s, respectively; Fig 5C).

Discussion

The lateral diffusion of a membrane protein reflects its molecular interactions in the membrane on the millisecond–second time scale (Cairo, *et al* 2006, Karnchanaphanurach, *et al* 2009). Here, we used single-particle tracking (SPT) to measure the lateral diffusion of individual GPC, band 3, and CD58 proteins in membranes of intact SAO RBCs and normal RBCs (nRBCs). These three proteins not only differ in function, but the molecular structures of the proteins also represent three different canonical types of membrane protein. GPC has a single transmembrane segment and a small intracellular domain; band 3 has multiple transmembrane segments and a large intracellular domain; and CD58 is a GPI-linked protein

with a large extracellular domain. Biochemical studies have shown that GPC molecules are an integral component of the junctional complex that couples the lipid bilayer to the RBC membrane skeleton (Gascard and Cohen 1994, Reid, *et al* 1989). Here, most of these molecules remain in a confined or tightly confined area over the entire period of experimental observation. Parallel studies showed that this type of diffusion is more likely to represent oscillatory diffusion of a tethered object than translational diffusion of an unattached object within a membrane corral (unpublished observation). The confinement size (area of oscillation) is smaller in SAO RBCs than in nRBCs. The smaller amplitude of oscillation in SAO RBCs is probably due to a stiffer membrane (see below). A small fraction of GPC molecules exhibits Brownian diffusion (11% in nRBCs and 6% in SAO RBCs), suggesting that some mobile GPC molecules could be required to maintain the dynamic flexibility of GPC-protein 4.1-actin junctions in the membrane.

Because SAO is a heterozygous disorder, SAO RBCs typically contain approximately 50% mutant band 3 molecules and 50% normal band 3 molecules (Bruce, *et al* 2000, Liu, *et al* 1990). In both SAO RBCs and nRBCs, BRIC6-laelled band 3 molecules showed confined motion over short times (<100 ms) and distances (<100 nm), and the area of confinement was smaller in SAO RBCs than in nRBCs. By using the parameter α to discriminate among three different modes of motion of band 3 populations over longer times (>1 s) and distances (>1 μm), we found that most band 3 molecules — 71% in nRBCs and 80% in SAO RBCs — showed confined motion or tightly confined motion during the 2-s period of experimental observation. In nRBCs, the degree of confinement is likely to depend on the molecular attachment of each individual band 3 molecule. Some band 3 molecules are a component of the GPC-4.1-actin complex, which is thought to bind up to 50% of the skeletally attached band 3 (Anong, *et al* 2009). These band 3 molecules are likely to be tightly confined due to the presence of about 6 spectrin tetramers attached to the same junctional complex (Boey, *et al* 1998). Other band 3 molecules are attached to the band 3-ankyrin complex; these molecules may be less tightly confined due to a higher degree of conformational freedom of the membrane skeleton at these locations. In SAO RBCs, the high-order linear band 3 oligomers appear to add a significant constraint to diffusion at the extracellular surface of the membrane, as virtually the entire confined population of band 3 molecules is shifted to the tightly confined population.

The fraction of band 3 molecules exhibiting Brownian diffusion is 29% in nRBCs but only 20% in SAO RBCs, probably reflecting the increased oligomeric state of band 3 molecules in SAO RBCs. These data are consistent with the results of FPR experiments in both nRBCs and SAO RBCs (Corbett and Golan 1993, Mohandas, *et al* 1992, Tsuji and Ohnishi 1986). In SAO RBCs, FPR experiments show a laterally mobile fraction of 16% of band 3 molecules (Liu, *et al* 1990) and polarized fluorescence depletion experiments show a rapidly rotating fraction of 15% of band 3 molecules (Liu, *et al* 1995), although some investigators have reported that no band 3 molecules exhibit long-range diffusion in SAO RBCs (Mohandas, *et al* 1992). By using single-particle tracking of a fluorescent marker that specifically labels normal band 3 molecules, Kodippili et al. (2009) reported that about half of band 3 molecules in both normal and SAO RBCs showed free diffusion. These interpretations may vary because of the different time scales and sampling rates of the various diffusion measurements. For example, Kodippili et al. (2009) found a high mobile fraction of band 3 molecules in experiments performed using a long observation time (8 s) and a low frame rate (120 fps), whereas Tomishige et al. (1998) reported a relatively large fraction of band 3 molecules undergoing “hop diffusion” over 10 s at a frame rate of 33 fps but mostly oscillatory motion of band 3 molecules within confinement areas of two different sizes in trajectories recorded for 67 ms (see discussion below).

Based on their measurements of the distribution of band 3 microdiffusion coefficients, Kodippili et al. (2009) have identified two populations of band 3 molecules in normal RBC membranes, 77% slowly diffusing and 23% more rapidly diffusing. In SAO RBCs, the slowly diffusing band 3 fraction represents 84% of the total and an even slower fraction of 16% is observed. The mean band 3 microdiffusion coefficients are 6.1×10^{-11} cm^2/s and 3.8×10^{-11} cm^2/s for normal and SAO RBCs, respectively. Using a substantially faster frame rate with 0.22-ms time resolution, Tomishige et al. (1998) reported a band 3 microdiffusion coefficient of 5.3×10^{-9} cm^2/s in normal RBC ghosts. Here, we measured band 3 microdiffusion coefficients of 7.6×10^{-10} cm^2/s and 3.9×10^{-10} cm^2/s in normal and SAO RBCs, respectively; these values are about 10-fold higher than those of Kodippili et al. (2009) but about 10-fold lower than those of Tomishige et al. (1998). These differences in the measured microdiffusion coefficients may be explained by differences in the rates at which band 3 position is sampled in the three experimental protocols, because, for confined diffusion, slower and slower microdiffusion coefficients would be expected the longer the duration over which the microdiffusion is sampled (see below). Nevertheless, the consistently reported twofold decrease in mean microdiffusion coefficients in SAO RBCs compared to nRBCs suggests the presence of additional constraints on band 3 lateral diffusion in SAO RBCs.

The mean values of the band 3 macrodiffusion coefficient measured here, 10.1×10^{-11} cm^2/s in normal RBCs and 3.4×10^{-11} cm^2/s in SAO RBCs, are also about 10-fold higher than those previously reported (Kodippili, *et al* 2009). In addition, each of the distributions of our macrodiffusion coefficients shows two populations of band 3 molecules. The mean values of our two (macrodiffusion) subpopulations are similar to the mean values of the microdiffusion coefficient for each of two band 3 populations described by Kodippili et al. (2009), suggesting that the 8-fold difference in frame rates between the two protocols may be responsible for the differences in the absolute values of the measured diffusion coefficients. At 33-ms time resolution, the band 3 macrodiffusion coefficient has been measured as 4.6×10^{-11} by single-particle tracking in normal RBC ghosts (Tomishige, *et al* 1998), which is in good agreement with our data and with data obtained using FPR (Corbett and Golan 1993, Mohandas, *et al* 1992, Tsuji and Ohnishi 1986).

About 50% of CD58 molecules show Brownian diffusion in nRBCs, and about 50% are confined or tightly confined. A remarkably higher degree of CD58 confinement is observed in SAO RBCs, and, like band 3, CD58 shows substantial compartmentalization in SAO RBC membranes. As noted above, band 3 forms high-order oligomers in SAO RBCs (Liu, *et al* 1995, Sarabia, *et al* 1993), and freeze-fracture electron microscopy reveals the linear nature of these band 3 aggregates (Liu, *et al* 1995). We hypothesize that the additional restriction on the motion of a GPI-linked protein like CD58 in SAO RBC membranes is due to membrane “corrals” formed by linear band 3 oligomers at the extracellular surface of the SAO RBC membrane. The patterns of the CD58 trajectories in SAO RBCs (Fig 5B) are consistent with compartmentalization of the membrane at the extracellular surface, and support the schematic model for diffusion constraints that is derived from band 3 motion in the RBC membrane (Fig 6).

The confinement size calculated from the trajectory of a diffusing membrane protein is an indicator of the extent and lateral distribution of obstacles to diffusion such as protein aggregates, membrane skeletal barriers, transient binding interactions, etc. Our method of determining the confinement size L does not distinguish between the oscillatory motion of a bound protein and the diffusive motion of a protein confined in a membrane compartment. Nonetheless, the confinement size of GPC, which is predominantly attached to the membrane skeleton, can be used to infer an effective stiffness constant of the RBC membrane. The stiffness constant is significantly increased in SAO RBCs compared to that

in nRBCs; this result is consistent with micropipette aspiration-based measurements of membrane stiffness in normal and SAO RBCs (Mohandas, *et al* 1992). At least some (perhaps all) of the oligomerized band 3 molecules are probably attached to the membrane skeleton in SAO RBCs, thereby contributing to the increased rigidity of the RBC membrane (Mohandas, *et al* 1992).

Unlike GPC trajectories, which show predominantly oscillatory motion due to attachment of the protein to the membrane skeleton, band 3 trajectories comprise a mixture of oscillatory and compartmentalized motion. Band 3 confinement sizes were 85–95 nm in nRBCs and 55–75 nm in SAO RBCs; these values are in agreement with previous reports (Tomishige, *et al* 1998). A different model has been used to calculate band 3 compartment sizes of about 40 nm and 70 nm in nRBCs and of solely 40 nm in SAO RBCs (Kodippili, *et al* 2009). These smaller values are similar to the standard deviation in the position of oscillating GPC molecules reported here and previously (Lee and Discher 2001), and have been interpreted as consistent with the motion of a membrane skeleton-tethered protein. Both our model and the model of Kodippili et al. (2009) suggest that band 3 confinement sizes are significantly smaller in SAO RBC membranes than in nRBC membranes.

The SAO mutation has been reported to protect against malaria morbidity (Genton, *et al* 1995), malaria invasion (Cortes, *et al* 2004, Hadley, *et al* 1983, Kidson, *et al* 1981), and malaria parasitaemia (Cattani, *et al* 1987), and may be correlated with a decreased incidence of cerebral malaria (Allen, *et al* 1999, Gallagher 2004, Lin, *et al* 2010). As we and others have suggested, the protective mechanism may involve increased rigidity of the SAO RBC membrane (Liu, *et al* 1995, Mohandas, *et al* 1984, Mohandas, *et al* 1992, Schofield, *et al* 1992b), which could potentially provide protection both by decreasing infected RBC adherence to vascular endothelium and by hindering parasite invasion of RBCs (Armah, *et al* 2005, Conroy, *et al* 2010, Cortes, *et al* 2005, Jakobsen, *et al* 1994, McCormick, *et al* 1997, Medana and Turner 2006). An alternative view has been presented by Dluzewski et al. (1992), who propose that *P. falciparum* invasion is high in fresh SAO RBCs and low in stored RBCs, which have low ATP levels. The effect of dehydration on *P. falciparum* invasion has also been discussed (Tiffert, *et al* 2005). Our results raise the possibility that restricted lateral diffusion of membrane proteins could contribute to the altered adherence of parasite-infected SAO RBCs to vascular endothelium. Further studies on the diffusion properties of proteins expressed by parasitized normal and SAO RBCs could help to elucidate the molecular pathology of *P. falciparum* invasion and parasitized RBC cytoadherence.

Supplementary Material

Refer to Web version on PubMed Central for supplementary material.

Acknowledgments

We thank Gloria Gonzales for coordinating blood sample collection. This work was supported by a grant from the National Institutes of Health, USA (HL032854 to DEG).

References

Allen S, O'Donnell A, Alexander N, Mgone C, Peto T, Clegg J, Alpers M, Weatherall D. Prevention of cerebral malaria in children in Papua New Guinea by southeast Asian ovalocytosis band 3. Am J Trop Med Hyg. 1999; 60:1056–1060. [PubMed: 10403343]

Anong WA, Franco T, Chu H, Weis TL, Devlin EE, Bodine DM, An X, Mohandas N, Low PS. Adducin forms a bridge between the erythrocyte membrane and its cytoskeleton and regulates membrane cohesion. Blood. 2009; 114:1904–1912. [PubMed: 19567882]

Armah H, Dodoo AK, Wiredu EK, Stiles JK, Adjei AA, Gyasi RK, Tettey Y. High-level cerebellar expression of cytokines and adhesion molecules in fatal, paediatric, cerebral malaria. Annals of Tropical Medicine and Parasitology. 2005; 99:629–647. [PubMed: 16212798]

Bennett V, Healy J. Organizing the fluid membrane bilayer: diseases linked to spectrin and ankyrin. Trends Mol Med. 2008; 14:28–36. [PubMed: 18083066]

Boey SK, Boal DH, Discher DE. Simulations of the erythrocyte cytoskeleton at large deformation. I. Microscopic models. Biophys J. 1998; 75:1573–1583. [PubMed: 9726958]

Bruce LJ, Tanner MJ. Erythroid band 3 variants and disease. Baillieres Best Pract Res Clin Haematol. 1999; 12:637–654. [PubMed: 10895257]

Bruce LJ, Wrong O, Toye AM, Young MT, Ogle G, Ismail Z, Sinha AK, McMaster P, Hwaihwanje I, Nash GB, Hart S, Lavu E, Palmer R, Othman A, Unwin RJ, Tanner MJ. Band 3 mutations, renal tubular acidosis and South-East Asian ovalocytosis in Malaysia and Papua New Guinea: loss of up to 95% band 3 transport in red cells. Biochem J. 2000; 350(Pt 1):41–51. [PubMed: 10926824]

Cairo CW, Mirchev R, Golan DE. Cytoskeletal regulation couples LFA-1 conformational changes to receptor lateral mobility and clustering. Immunity. 2006; 25:297–308. [PubMed: 16901728]

Casey JR, Reithmeier RA. Analysis of the oligomeric state of Band 3, the anion transport protein of the human erythrocyte membrane, by size exclusion high performance liquid chromatography. Oligomeric stability and origin of heterogeneity. J Biol Chem. 1991; 266:15726–15737. [PubMed: 1874731]

Cattani JA, Gibson FD, Alpers MP, Crane GG. Hereditary ovalocytosis and reduced susceptibility to malaria in Papua New Guinea. Transactions of the Royal Society of Tropical Medicine and Hygiene. 1987; 81:705–709. [PubMed: 3329776]

Chasis JA, Mohandas N. Erythrocyte membrane deformability and stability: two distinct membrane properties that are independently regulated by skeletal protein associations. J Cell Biol. 1986; 103:343–350. [PubMed: 3733870]

Conroy AL, Phiri H, Hawkes M, Glover S, Mallewa M, Seydel KB, Taylor TE, Molyneux ME, Kain KC. Endothelium-Based Biomarkers Are Associated with Cerebral Malaria in Malawian Children: A Retrospective Case-Control Study. PLoS ONE. 2010; 5:e15291. [PubMed: 21209923]

Corbett JD, Golan DE. Band 3 and glycophorin are progressively aggregated in density-fractionated sickle and normal red blood cells. Evidence from rotational and lateral mobility studies. J Clin Invest. 1993; 91:208–217. [PubMed: 8423219]

Corbett JD, Agre P, Palek J, Golan DE. Differential control of band 3 lateral and rotational mobility in intact red cells. J Clin Invest. 1994; 94:683–688. [PubMed: 8040322]

Cortes A, Benet A, Cooke BM, Barnwell JW, Reeder JC. Ability of Plasmodium falciparum to invade Southeast Asian ovalocytes varies between parasite lines. Blood. 2004; 104:2961–2966. [PubMed: 15265796]

Cortes A, Mellombo M, Mgone CS, Beck HP, Reeder JC, Cooke BM. Adhesion of Plasmodium falciparum-infected red blood cells to CD36 under flow is enhanced by the cerebral malaria-protective trait South-East Asian ovalocytosis. Mol Biochem Parasitol. 2005; 142:252–257. [PubMed: 15978955]

Dluzewski AR, Nash GB, Wilson RJ, Reardon DM, Gratzer WB. Invasion of hereditary ovalocytes by Plasmodium falciparum in vitro and its relation to intracellular ATP concentration. Mol Biochem Parasitol. 1992; 55:1–7. [PubMed: 1435863]

Feder TJ, Brust-Mascher I, Slattery JP, Baird B, Webb WW. Constrained diffusion or immobile fraction on cell surfaces: a new interpretation. Biophys J. 1996; 70:2767–2773. [PubMed: 8744314]

Gallagher PG. Hereditary elliptocytosis: spectrin and protein 4.1R. Seminars in Hematology. 2004; 41:142–164. [PubMed: 15071791]

Gascard P, Cohen CM. Absence of high-affinity band 4.1 binding sites from membranes of glycophorin C- and D-deficient (Leach phenotype) erythrocytes. Blood. 1994; 83:1102–1108. [PubMed: 8111049]

Genton B, al-Yaman F, Mgone CS, Alexander N, Paniu MM, Alpers MP, Mokela D. Ovalocytosis and cerebral malaria. Nature. 1995; 378:564–565. [PubMed: 8524388]

Groves JD, Ring SM, Schofield AE, Tanner MJ. The expression of the abnormal human red cell anion transporter from South-East Asian ovalocytes (band 3 SAO) in Xenopus oocytes. FEBS Lett. 1993; 330:186–190. [PubMed: 7689982]

Guizouarn H, Borgese F, Gabillat N, Harrison P, Goede JS, McMahon C, Stewart GW, Bruce LJ. South-east Asian ovalocytosis and the cryohydrocytosis form of hereditary stomatocytosis show virtually indistinguishable cation permeability defects. Br J Haematol. 2011; 152:655–664. [PubMed: 21255002]

Hadley T, Saul A, Lamont G, Hudson DE, Miller LH, Kidson C. Resistance of Melanesian elliptocytes (ovalocytes) to invasion by Plasmodium knowlesi and Plasmodium falciparum malaria parasites in vitro. J Clin Invest. 1983; 71:780–782. [PubMed: 6338046]

Jakobsen PH, Morris-Jones S, Ronn A, Hviid L, Theander TG, Elhassan IM, Bygbjerg IC, Greenwood BM. Increased plasma concentrations of sICAM-1, sVCAM-1 and sELAM-1 in patients with Plasmodium falciparum or P. vivax malaria and association with disease severity. Immunology. 1994; 83:665–669. [PubMed: 7533138]

Johnson, NL.; Kotz, S.; Balakrishnan, N. Continuous univariate distributions. John Wiley& Sons, Inc; New York: 1994.

Karnchanaphanurach P, Mirchev R, Ghiran I, Asara JM, Papahadjopoulos-Sternberg B, Nicholson-Weller A, Golan DE. C3b deposition on human erythrocytes induces the formation of a membrane skeleton-linked protein complex. J Clin Invest. 2009; 119:788–801. [PubMed: 19258706]

Kay MM. Band 3 and its alterations in health and disease. Cell Mol Biol (Noisy-le-grand). 2004; 50:117–138. [PubMed: 15095783]

Khan AA, Hanada T, Mohseni M, Jeong JJ, Zeng L, Gaetani M, Li D, Reed BC, Speicher DW, Chishti AH. Dematin and adducin provide a novel link between the spectrin cytoskeleton and human erythrocyte membrane by directly interacting with glucose transporter-1. J Biol Chem. 2008; 283:14600–14609. [PubMed: 18347014]

Kidson C, Lamont G, Saul A, Nurse GT. Ovalocytic erythrocytes from Melanesians are resistant to invasion by malaria parasites in culture. Proc Natl Acad Sci U S A. 1981; 78:5829–5832. [PubMed: 7029547]

Kodippili GC, Spector J, Sullivan C, Kuypers FA, Labotka R, Gallagher PG, Ritchie K, Low PS. Imaging of the diffusion of single band 3 molecules on normal and mutant erythrocytes. Blood. 2009; 113:6237–6245. [PubMed: 19369229]

Kuma H, Abe Y, Askin D, Bruce LJ, Hamasaki T, Tanner MJ, Hamasaki N. Molecular basis and functional consequences of the dominant effects of the mutant band 3 on the structure of normal band 3 in Southeast Asian ovalocytosis. Biochemistry. 2002; 41:3311–3320. [PubMed: 11876639]

Kusumi A, Sako Y, Yamamoto M. Confined lateral diffusion of membrane receptors as studied by single particle tracking (nanovid microscopy). Effects of calcium-induced differentiation in cultured epithelial cells. Biophys J. 1993; 65:2021–2040. [PubMed: 8298032]

Lee JC, Discher DE. Deformation-enhanced fluctuations in the red cell skeleton with theoretical relations to elasticity, connectivity, and spectrin unfolding. Biophys J. 2001; 81:3178–3192. [PubMed: 11720984]

Lin E, Tavul L, Michon P, Richards JS, Dabod E, Beeson JG, King CL, Zimmerman PA, Mueller I. Minimal Association of Common Red Blood Cell Polymorphisms with Plasmodium falciparum Infection and Uncomplicated Malaria in Papua New Guinean School Children. Am J Trop Med Hyg. 2010; 83:828–833. [PubMed: 20889874]

Liu SC, Palek J, Yi SJ, Nichols PE, Derick LH, Chiou SS, Amato D, Corbett JD, Cho MR, Golan DE. Molecular basis of altered red blood cell membrane properties in Southeast Asian ovalocytosis: role of the mutant band 3 protein in band 3 oligomerization and retention by the membrane skeleton. Blood. 1995; 86:349–358. [PubMed: 7795244]

Liu SC, Zhai S, Palek J, Golan DE, Amato D, Hassan K, Nurse GT, Babona D, Coetzer T, Jarolim P, Zaik M, Borwein S. Molecular defect of the band 3 protein in southeast Asian ovalocytosis. N Engl J Med. 1990; 323:1530–1538. [PubMed: 2146504]

Lux, SE.; Palek, J. Disorders of the red blood cell membrane. In: Handin, RI.; Lux, SE.; Stossel, TP., editors. Blood: Principles and Practice of Hematology. Lippincott Williams & Wilkins; Philadelphia, PA: 2003. p. 1709-1859.

McCormick CJ, Craig A, Roberts D, Newbold CI, Berendt AR. Intercellular adhesion molecule-1 and CD36 synergize to mediate adherence of Plasmodium falciparum-infected erythrocytes to cultured human microvascular endothelial cells. J Clin Invest. 1997; 100:2521–2529. [PubMed: 9366566]

Medana IM, Turner GDH. Human cerebral malaria and the blood-brain barrier. International Journal for Parasitology. 2006; 36:555–568. [PubMed: 16616145]

Mirchev R, Golan DE. Single-particle tracking and laser optical tweezers studies of the dynamics of individual protein molecules in membranes of intact human and mouse red cells. Blood Cells Mol Dis. 2001; 27:143–147. [PubMed: 11358375]

Mohandas N, Lie-Injo LE, Friedman M, Mak JW. Rigid membranes of Malayan ovalocytes: a likely genetic barrier against malaria. Blood. 1984; 63:1385–1392. [PubMed: 6722355]

Mohandas N, Winardi R, Knowles D, Leung A, Parra M, George E, Conboy J, Chasis J. Molecular basis for membrane rigidity of hereditary ovalocytosis. A novel mechanism involving the cytoplasmic domain of band 3. J Clin Invest. 1992; 89:686–692. [PubMed: 1737855]

Moriyama R, Ideguchi H, Lombardo CR, Van Dort HM, Low PS. Structural and functional characterization of band 3 from Southeast Asian ovalocytes. J Biol Chem. 1992; 267:25792–25797. [PubMed: 1464593]

Murphy SC, Samuel BU, Harrison T, Speicher KD, Speicher DW, Reid ME, Prohaska R, Low PS, Tanner MJ, Mohandas N, Haldar K. Erythrocyte detergent-resistant membrane proteins: their characterization and selective uptake during malarial infection. Blood. 2004; 103:1920–1928. [PubMed: 14592818]

Reid ME, Takakuwa Y, Tchernia G, Jensen RH, Chasis JA, Mohandas N. Functional role for glycophorin C and its interaction with the human red cell membrane skeletal component, protein 4.1. Prog Clin Biol Res. 1989; 319:553–571. discussion 572–553. [PubMed: 2622928]

Salomao M, Zhang X, Yang Y, Lee S, Hartwig JH, Chasis JA, Mohandas N, An X. Protein 4.1R-dependent multiprotein complex: new insights into the structural organization of the red blood cell membrane. Proc Natl Acad Sci U S A. 2008; 105:8026–8031. [PubMed: 18524950]

Sarabia VE, Casey JR, Reithmeier RA. Molecular characterization of the band 3 protein from Southeast Asian ovalocytes. J Biol Chem. 1993; 268:10676–10680. [PubMed: 8486716]

Saxton MJ. Single-particle tracking: effects of corrals. Biophys J. 1995; 69:389–398. [PubMed: 8527652]

Schofield AE, Reardon DM, Tanner MJ. Defective anion transport activity of the abnormal band 3 in hereditary ovalocytic red blood cells. Nature. 1992a; 355:836–838. [PubMed: 1538763]

Schofield AE, Tanner MJA, Pinder JC, Clough B, Bayley PM, Nash GB, Dluzewski AR, Reardon DM, Cox TM, Wilson RJM, Gratzer WB. Basis of unique red cell membrane properties in hereditary ovalocytosis. Journal of Molecular Biology. 1992b; 223:949–958. [PubMed: 1538405]

Smythe JS, Spring FA, Gardner B, Parsons SF, Judson PA, Anstee DJ. Monoclonal antibodies recognizing epitopes on the extracellular face and intracellular N-terminus of the human erythrocyte anion transporter (band 3) and their application to the analysis of South East Asian ovalocytes. Blood. 1995; 85:2929–2936. [PubMed: 7742553]

Tiffert T, Lew VL, Ginsburg H, Krugliak M, Croisille L, Mohandas N. The hydration state of human red blood cells and their susceptibility to invasion by Plasmodium falciparum. Blood. 2005; 105:4853–4860. [PubMed: 15728121]

Tomishige M, Sako Y, Kusumi A. Regulation mechanism of the lateral diffusion of band 3 in erythrocyte membranes by the membrane skeleton. J Cell Biol. 1998; 142:989–1000. [PubMed: 9722611]

Tsuji A, Ohnishi S. Restriction of the lateral motion of band 3 in the erythrocyte membrane by the cytoskeletal network: dependence on spectrin association state. Biochemistry. 1986; 25:6133–6139. [PubMed: 3790510]

Wang DN. Band 3 protein: structure, flexibility and function. FEBS Lett. 1994; 346:26–31. [PubMed: 8206153]

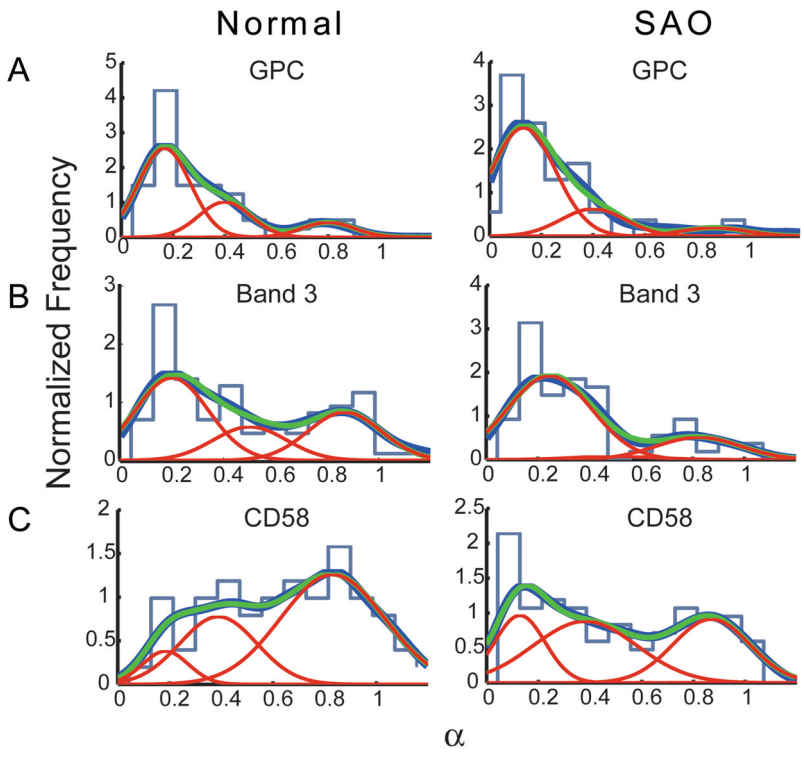

Fig 1.

Distributions of α values. (A) GPC; (B) band 3; (C) CD58. **Light blue** curve, histogram of experimental data; **dark** blue curve, envelope smoothing function of experimental data; red curves, Gaussian best-fit curves describing deconvolved populations; green curve, sum of the red curves.

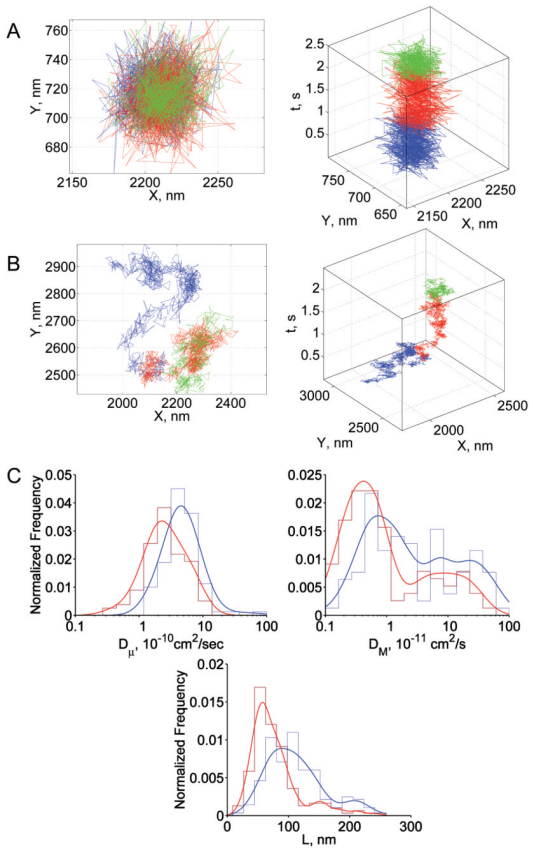

Fig 2.

Summary of GPC results. (A) Representative trajectory from the tightly confined fraction **in normal and SAO RBCs**; (B) representative trajectory from the confined fraction **in normal and SAO RBCs**; (C) diffusion parameter distributions: blue, normal RBCs; red, SAO RBCs. In panels A and B, blue, red, and green steps represent the initial, middle, and terminal portions of the trajectory, respectively. In panel C, envelope smoothing functions are overlaid on histograms of experimental data.

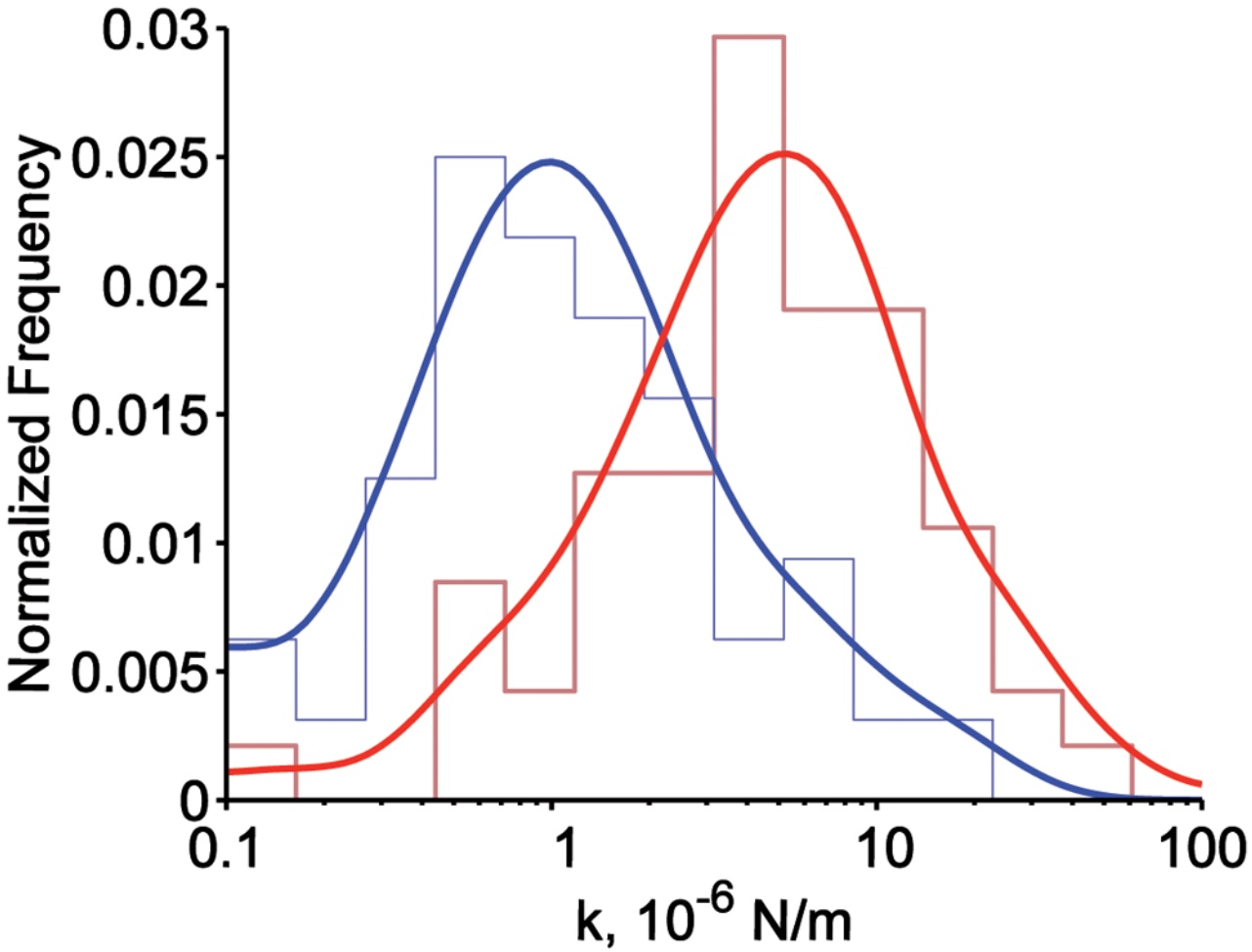

Fig 3.

Distribution of the effective spring constant k_{eff} of the RBC membrane. Blue, normal RBCs; red, SAO RBCs. For both distributions, envelope smoothing functions are overlaid on histograms of experimental data.

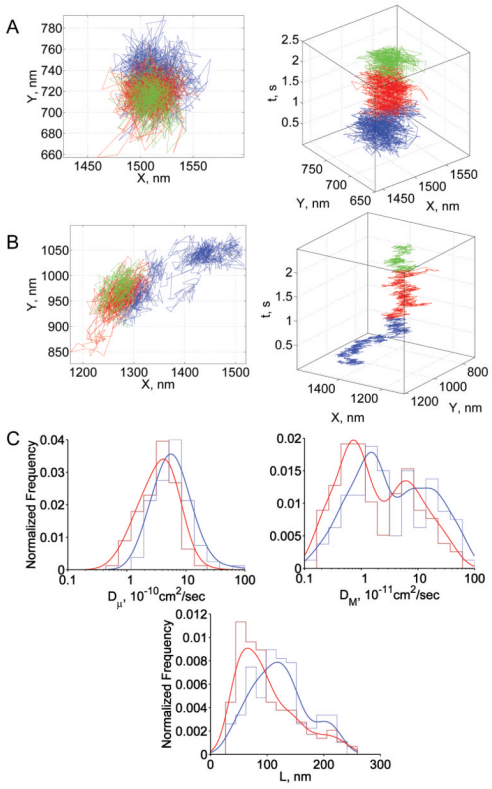

Fig 4.

Summary of band 3 results. (A) Representative trajectory from the tightly confined fraction **in normal and SAO RBCs**; (B) representative trajectory from the confined fraction **in normal and SAO RBCs**; (C) diffusion parameter distributions: blue, normal RBCs; red, SAO RBCs. In panels A and B, blue, red, and green steps represent the initial, middle, and terminal portions of the trajectory, respectively. In panel C, envelope smoothing functions are overlaid on histograms of experimental data.

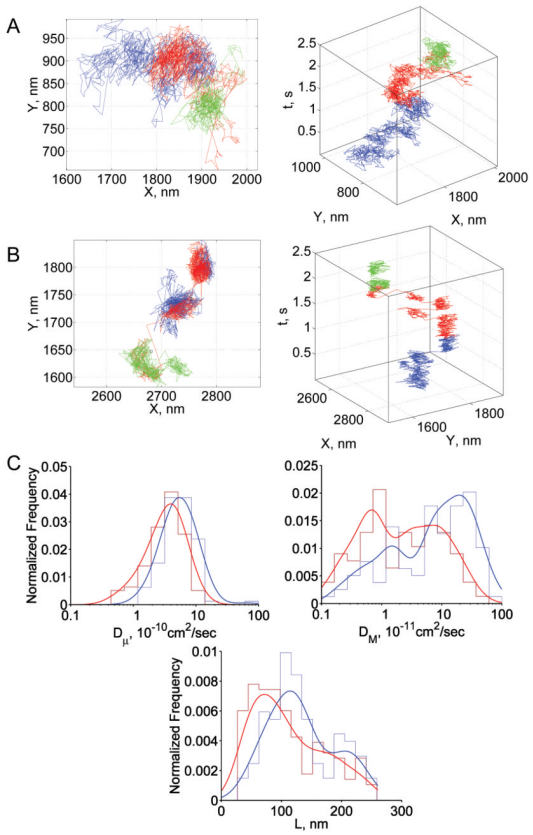

Fig 5.

Summary of CD58 results. (A) Representative trajectory in normal RBCs; (B) representative trajectory in SAO RBCs; (C) diffusion parameter distributions: blue, normal RBCs; red, SAO RBCs; L was calculated only from trajectories showing confined or tightly confined motion. In panels A and B, blue, red, and green steps represent the initial, middle, and terminal portions of the trajectory, respectively. In panel C, envelope smoothing functions are overlaid on histograms of experimental data.

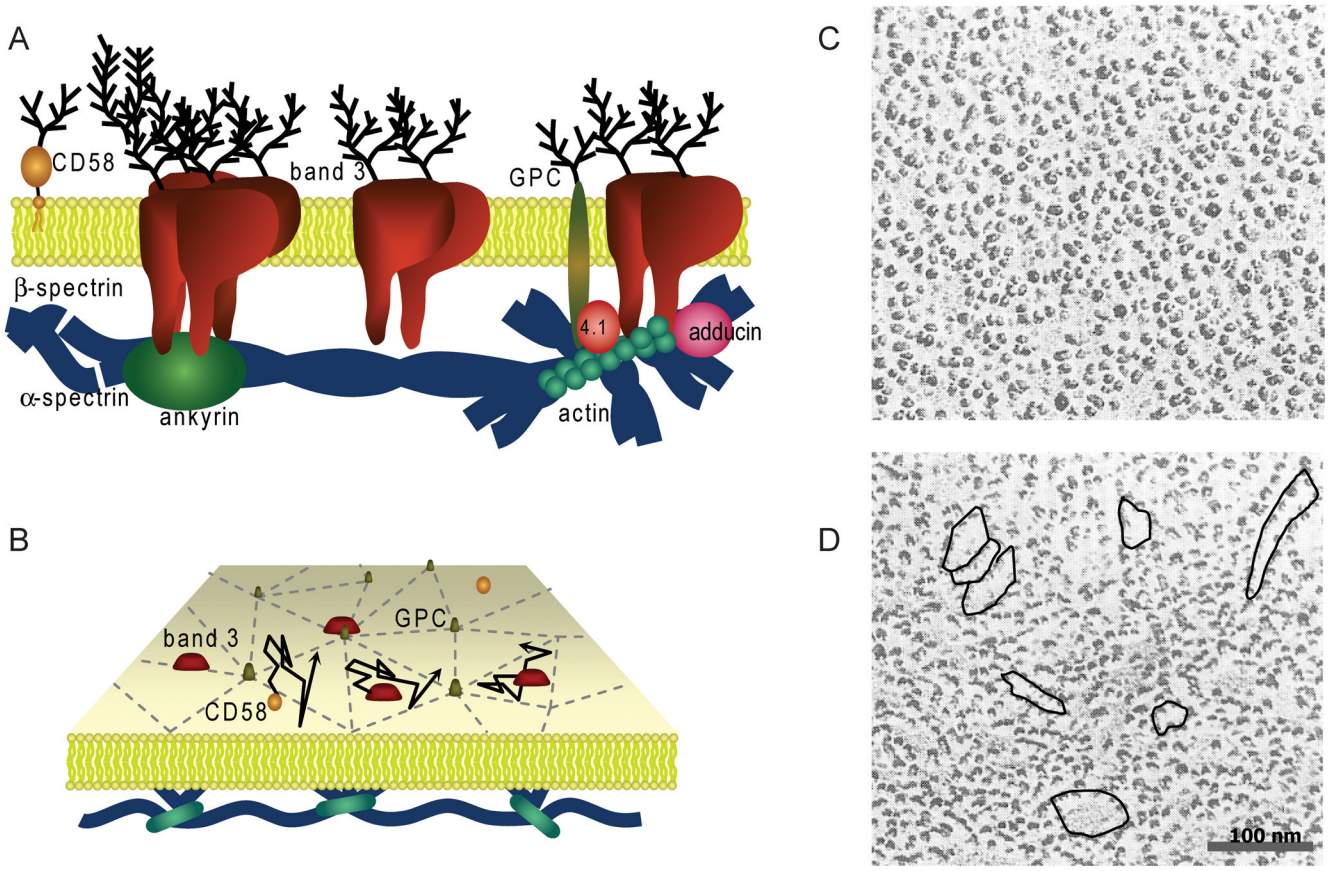

Fig 6.

Compartmentalization of RBC membrane. (A) Schematic diagram of RBC membrane depicting some important integral membrane proteins and membrane skeletal proteins. (B) Perspective view of the membrane showing the compartmentalization of GPC and band 3 diffusion due to the membrane skeleton. (C-D) Freeze-fracture electron micrographs of the outer face of a normal RBC membrane (C) and an SAO RBC membrane (D;. In panel D, overlaid are regions of **potential** extracellular compartmentalization due to linear band 3 oligomers in the SAO RBC membrane. These extracellular compartments could provide additional restriction on CD58 diffusion in SAO RBCs. Scale bar, 100 nm. The research in panel D was originally published in *Blood*. Liu, S.C., Palek, J., Yi, S.J., Nichols, P.E., Derick, L.H., Chiou, S.S., Amato, D., Corbett, J.D., Cho, M.R. & Golan, D.E. (1995) Molecular basis of altered red blood cell membrane properties in Southeast Asian ovalocytosis: role of the mutant band 3 protein in band 3 oligomerization and retention by the membrane skeleton. *Blood*, **86**, 349–358. © the American Society of Hematology

Table 1

Populations and confinement sizes of GPC trajectories in normal and SAO RBCs

RBCs	Population Peak	Mean α	Confinement Size (L), nm, ± SEM	Fraction of Trajectories
Normal (n=47)	1	0.17	62 ± 7	64%
	2	0.40	90 ± 3	25%
	3	0.78	*	11%
SAO (n=63)	1	0.14	53 ± 3	77%
	2	0.41	63 ± 2	17%
	3	0.86	*	6%

Table 2

Populations and confinement sizes of band 3 trajectories in normal and SAO RBCs

RBCs	Population Peak	Mean α	Confinement Size (L), nm, ± SEM	Fraction of Trajectories
Normal (n=100)	1	0.20	84 ± 9	50%
	2	0.50	97 ± 4	21%
	3	0.87	*	29%
SAO (n=63)	1	0.19	53 ± 4	77%
	2	0.39	73 ± 3	3%
	3	0.83	*	20%

Table 3

Populations and confinement sizes of CD58 trajectories in normal and SAO RBCs

RBCs	Population Peak	Mean α	Confinement Size (L), nm, ± SEM	Fraction of Trajectories
Normal (n=59)	1	0.26	75 ± 15	27%
	2	0.50	106 ± 7	25%
	3	0.89	*	48%
SAO (n=98)	1	0.17	70 ± 5	44%
	2	0.50	95 ± 7	23%
	3	0.87	*	33%